JOURNAL OF GEOPHYSICAL RESEARCH, VOL. 100, NO. A12, PAGES 23,993–24,002, DECEMBER 1, 1995

Gravity waves near 300 km over the polar caps

F. S. Johnson, W. B. Hanson,[1] R. R. Hodges, and W. R. Coley

Center for Space Sciences, The University of Texas at Dallas, Richardson

034752

G. R. Carignan

The University of Michigan, Ann Arbor

N. W. Spencer

NASA Goddard Space Flight Center, Greenbelt, Maryland

Abstract. Distinctive wave forms in the distributions of vertical velocity and temperature of both neutral particles and ions are frequently observed from Dynamics Explorer 2 at altitudes above 250 km over the polar caps. These are interpreted as being due to internal gravity waves propagating in the neutral atmosphere. The disturbances are characterized by vertical velocity perturbations of the order of 100 m/s and horizontal wave lengths along the satellite path of about 500 km. They often extend across the entire polar cap. The associated temperature perturbations indicate that the horizontal phase progression is from the nightside to the dayside. Vertical displacements are inferred to be of the order of 10 km and the periods to be of the order of 10^3 s. The waves must propagate in the neutral atmosphere, but they usually are most clearly recognizable in the observations of ion vertical velocity and ion temperature. By combining the neutral pressure calculated from the observed neutral concentration and temperature with the vertical component of the neutral velocity, an upward energy flux of the order of 0.04 erg/cm^2-s at 250 km has been calculated, which is about equal to the maximum total solar ultraviolet heat input above that altitude. Upward energy fluxes calculated from observations on orbital passes at altitudes from 250 to 560 km indicate relatively little attenuation with altitude.

Introduction

The purpose of this paper is to describe some wave motions observed over the polar caps at altitudes in excess of 250 km using Dynamics Explorer 2 (DE 2) data from the ion drift meter (IDM) [*Heelis et al.*, 1981], the retarding potential analyzer (RPA) [*Hanson et al.*, 1981], the wind and temperature mass spectrometer (WATS) [*Spencer et al.*, 1981], and the neutral atmosphere composition spectrometer (NACS) [*Carignan et al.*, 1981]. The waveforms are interpreted as being due to internal gravity waves propagating in the neutral atmosphere. The motions are seen as well-formed, quasi-sinusoidal patterns of vertical velocity (both ion and neutral) with associated temperature and composition perturbations that permit evaluation of some properties of the waves; these patterns indicate that the horizontal phase progression of the waves is from the nightside to the dayside and that the waves transport significant amounts of energy upwards, even at altitudes as high as the base of the exosphere. Waves of this sort have been observed over much of the Earth by *Potter et al.* [1976], who described their distribution with latitude and possible causes. *Gross and Huang* [1985] have observed waves of similar wavelength at low to middle latitudes and altitudes near 250 km.

The observation of internal gravity waves at altitudes as high as the exobase was unexpected because of anticipated strong attenuation above 120 km due to viscosity and thermal conduction. The expectation of strong absorption is based on the work of *Pitteway and Hines* [1963], *Midgley and Liemohn* [1966], and *Hodges* [1969].

Wave forms are illustrated in Figure 1 for propagating and standing waves; it will be useful to keep these patterns in mind in the subsequent discussion of the observations. The displacements from equilibrium positions and the velocities associated with the changing displacements are portrayed. In the present context the displacements and velocities are the components in the vertical direction. From satellites, neither the displacements nor the time variations at fixed points in space can be observed directly because of the motion of the satellite. The satellite observations constitute nearly a snapshot at a fixed time because the satellite velocity is so high compared to the wave propagation velocity; that is, the observations are essentially of spatial variations. The vertical displacement perturbations can be inferred from the temperature perturbations or from composition changes. The displacements and velocity perturbations are in phase quadrature in time for both propagating and standing waves. For propagating waves the perturbations are also in phase quadrature in space, and the displacement profiles lead or lag the velocity profiles depending upon whether the coordinate axis is in the direction of wave propagation or opposed to it. In the case of standing waves the spatial profiles are in phase half the time and out of phase half the time, and no perturbations occur at the nodes, as illustrated in Figure 1.

[1]Deceased September 11, 1994.

Paper number 95JA02858
0148-0227/95/95JA-02858$05.00

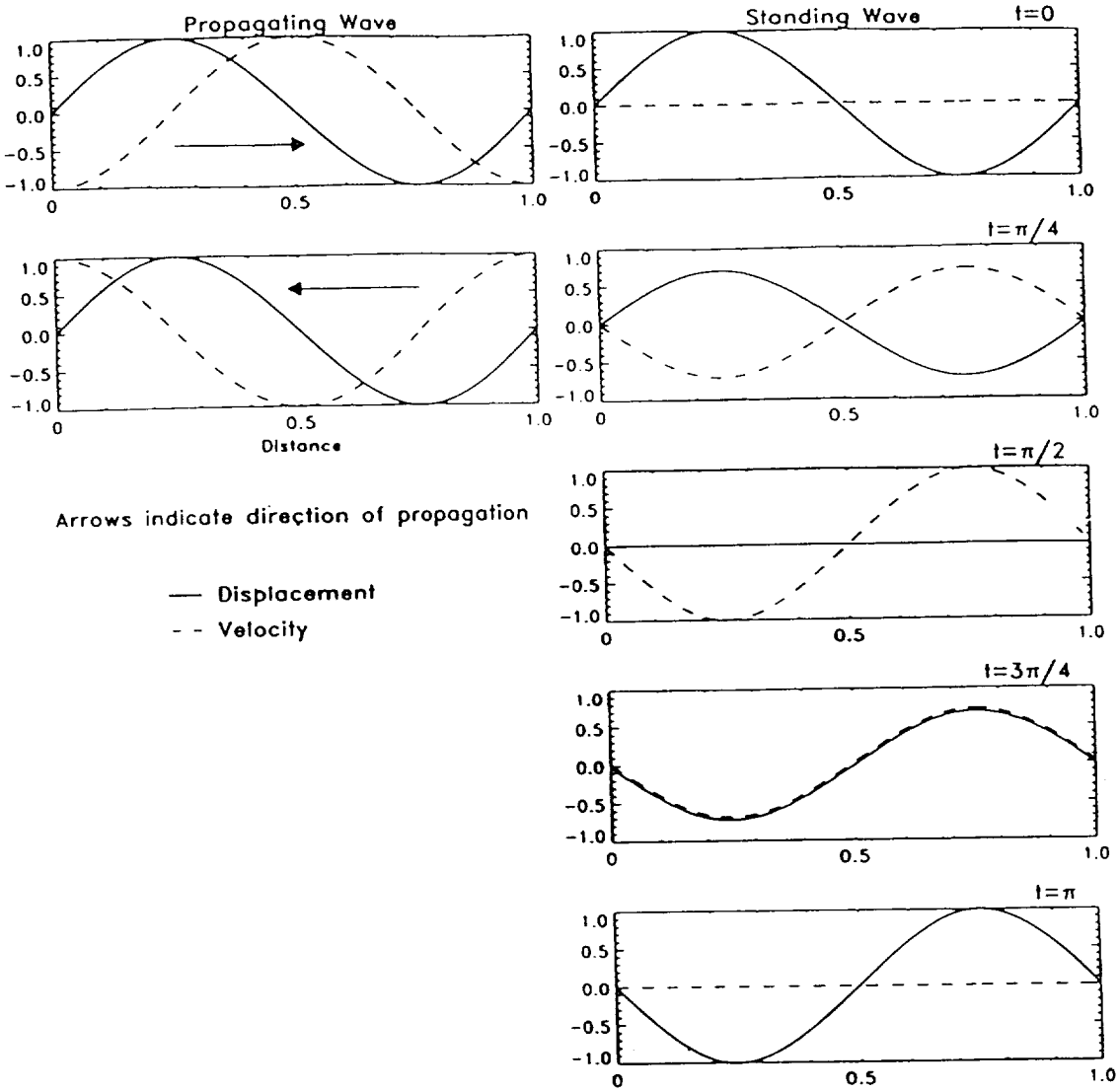

Figure 1. The spatial distribution of displacements and velocities for propagating waves and for standing waves at five selected time intervals. At selected instants in time the velocities and displacements for standing waves are either in phase (e.g., for $\pi/2 < t < \pi$) or in antiphase (e.g., for $0 < t < \pi/2$) with one another.

Observations

Figure 2 shows the wave perturbations seen in the vertical ion drifts observed by the IDM on 22 orbital passes over a polar cap. Seven-thousand-kilometer (15-min) orbital segments are shown, the arbitrarily selected start times being indicated in each panel; the time intervals have been chosen so that the segments are located over a polar cap. (In three cases the initial portion of the segment is missing.) The K_p magnetic indices are shown in each panel; there is no obvious relationship between occurrence of these waves and the K_p index. However, the interplanetary field was directed southward during 33 out of 40 passes on which waves were observed and interplanetary field data were available. The vertical velocity perturbation amplitudes vary from about 100 to 300 m/s; other records show smaller amplitudes. Although not shown in Figure 2, velocity-correlated ion temperature perturbations were present in each case, and these could be used to determine whether the horizontal wave progression had a component in the direction of satellite motion or opposed to it.

Figure 3 shows IDM data for ion velocity components and RPA data for ion temperatures and concentrations from orbit 8303 on February 1, 1983; the spacecraft altitude was about 253 km. The oscillations in question extend virtually across the entire polar cap. The satellite entered the polar cap near local magnetic noon, at 1613:35 UT, and exited near 0300 MLT, at 1621:09 UT. The waves are seen most clearly in terms of the vertical ion velocities, v_y. Because the magnetic field is almost vertical, ion motions in the horizontal are severely constrained and it is no surprise that no evidence of wave motions can be seen in the horizontal ion velocity components v_x along the orbit or v_z across the orbit. Ion temperature measurements are shown in the top panel and the oscillations are clearly evident as perturbations of the ion temperature. Ion concentrations are shown in the second panel, but they show little or no evidence of the oscillations, and this is usually the case in other records.

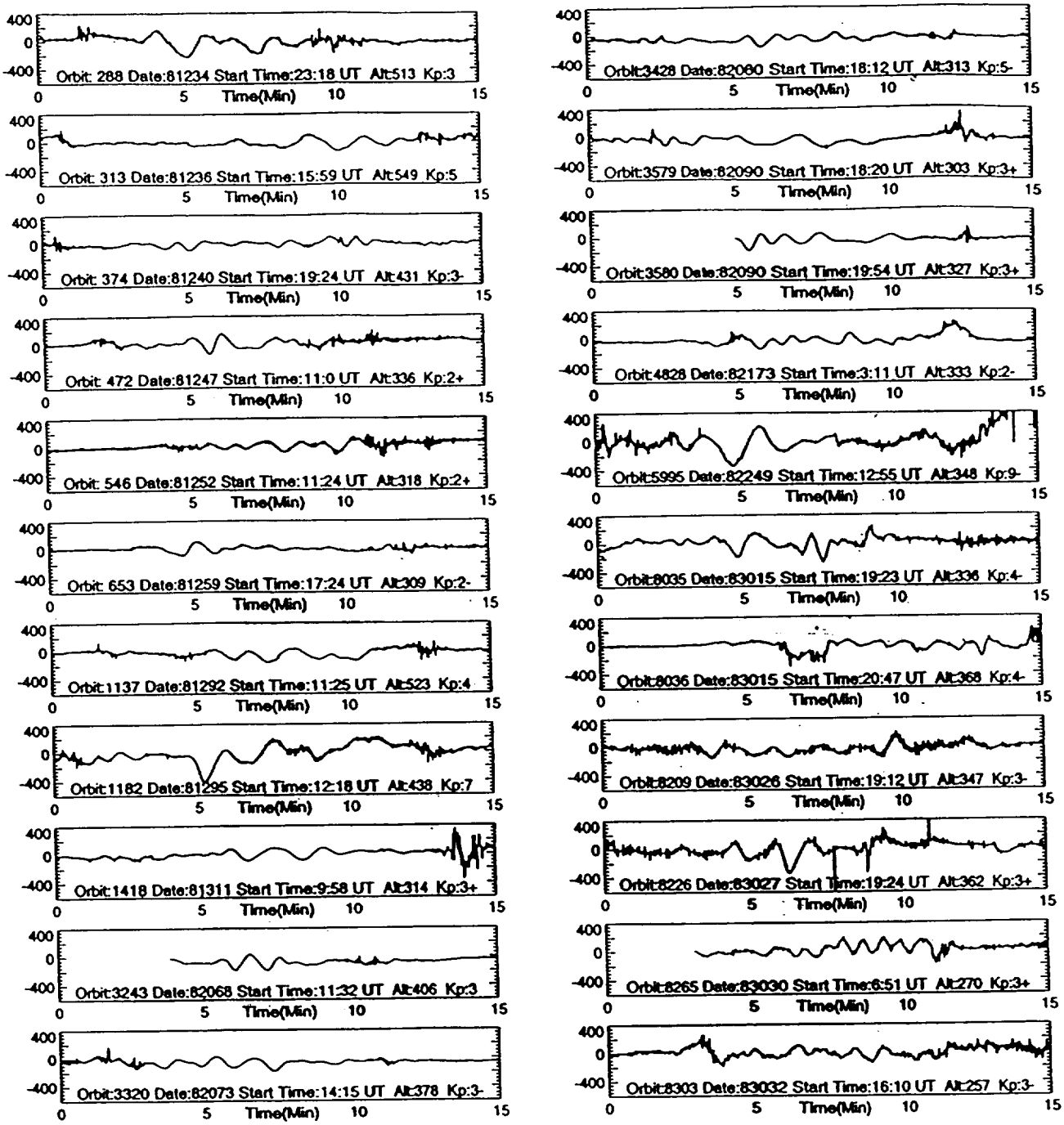

Figure 2. A selection of records from the ion drift meter on DE 2 showing periodic vertical velocity perturbations at altitudes of 250 km and above. The orbit number, date, UT at the beginning of the record, altitude at the beginning of the record, and K_p index are all shown. The ordinate scale is vertical ion velocity in meters per second.

Figure 4 shows the same ion vertical velocity and ion temperature records shown in Figure 3, but for the time interval 1614:34 to 1621:14 UT, along with the cross correlation between them. The record consists of 400 observations; the abscissa scale for the middle panel is the serial number of the individual observations. The scale for the top panel is the displacement to the right of the ion velocity data relative to the ion temperature data in units of the interval between observations. (Positive values are referred to as "lead".) To make the cross-correlation computation, the observations were first converted to perturbation values by taking differences from the straight, dotted detrend lines shown running through the observations.

The correlation is greatest for a lag of 11.5 intervals. Taking the shifts for the adjoining peaks in the correlation function (−65 and +40) as indicative of twice the wavelength, the average wavelength along the satellite path is 53.5 intervals (that is, 53.5 seconds or 414 km). Thus the effective phase shift between ion velocity and temperature is (11.5/53.5)360° = 79°, or nearly 90°. Simply overlaying the

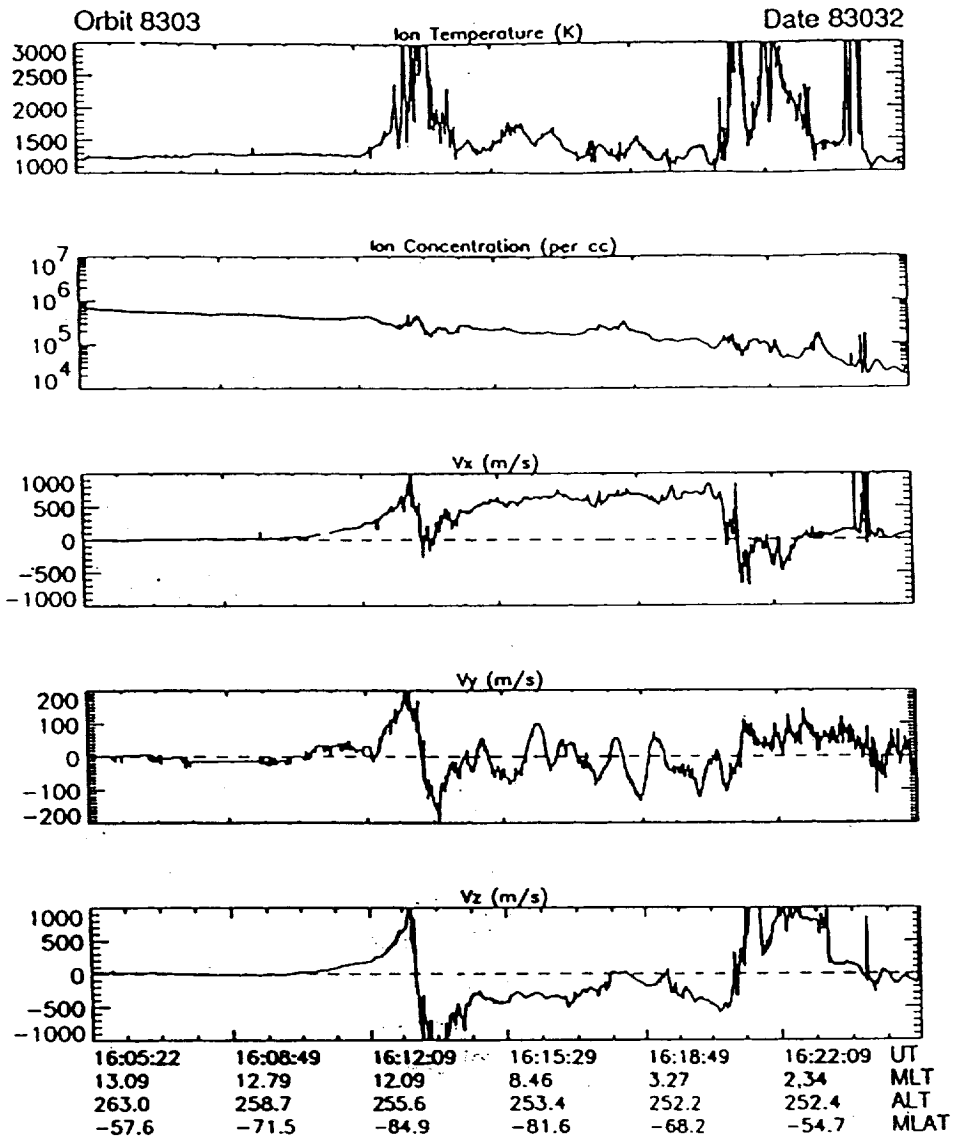

Figure 3. Ion temperatures, concentrations, and velocity components observed from DE 2 on orbit 8303 on February 1, 1983. The abscissa labels apply to the tic marks at the left-hand ends of the labels. The x axis is along the direction of motion of the satellite, the y axis is upwards, and the z axis is perpendicular to the orbit plane. Observations are plotted at 1-s (7.74-km) intervals.

records in the two lower panels also demonstrates clearly that the phase difference is about 90°. The exact value of the phase shift is not used in the analysis of the vertical component of energy flow described below; the phase difference is used only to determine whether the horizontal phase progression of the waves has a component in the direction of satellite motion or opposed to it.

Because of the predominance of neutrals over ions, the waves must propagate in the neutral atmosphere and the motions of the ions are driven by the neutral motions. We assume that the temperature perturbations have their maximum positive values at points of maximum downward displacement and thus maximum adiabatic heating. The ion temperature perturbations are simply a reflection of the neutral temperature perturbations to which they are closely coupled at the altitude of observation. Near the points of maximum downward displacement, the upward vertical velocities must be near zero and increasing with time. The phasing in Figure 4, the upward vertical velocity profile lagging the temperature perturbation profile, indicates that the horizontal phase progression has a component in the direction opposite to that of the satellite motion. As the satellite motion in this case was from the dayside to the nightside, the direction of horizontal wave propagation is from the nightside to the dayside.

Figure 5 shows the cross correlation between neutral vertical velocity and neutral temperature perturbations. In this case the observation interval was 8 s, so only 50 observations are available during the 400-s period of observation. The perturbation values were evaluated in terms of the differences from the best-fit dotted detrend lines shown in the figure. The cross correlation is very similar to that for the ion temperatures and vertical velocities shown in Figure 4; the average phase shift in this case is 95°.

At the satellite altitude of about 250 km the ion and neutral

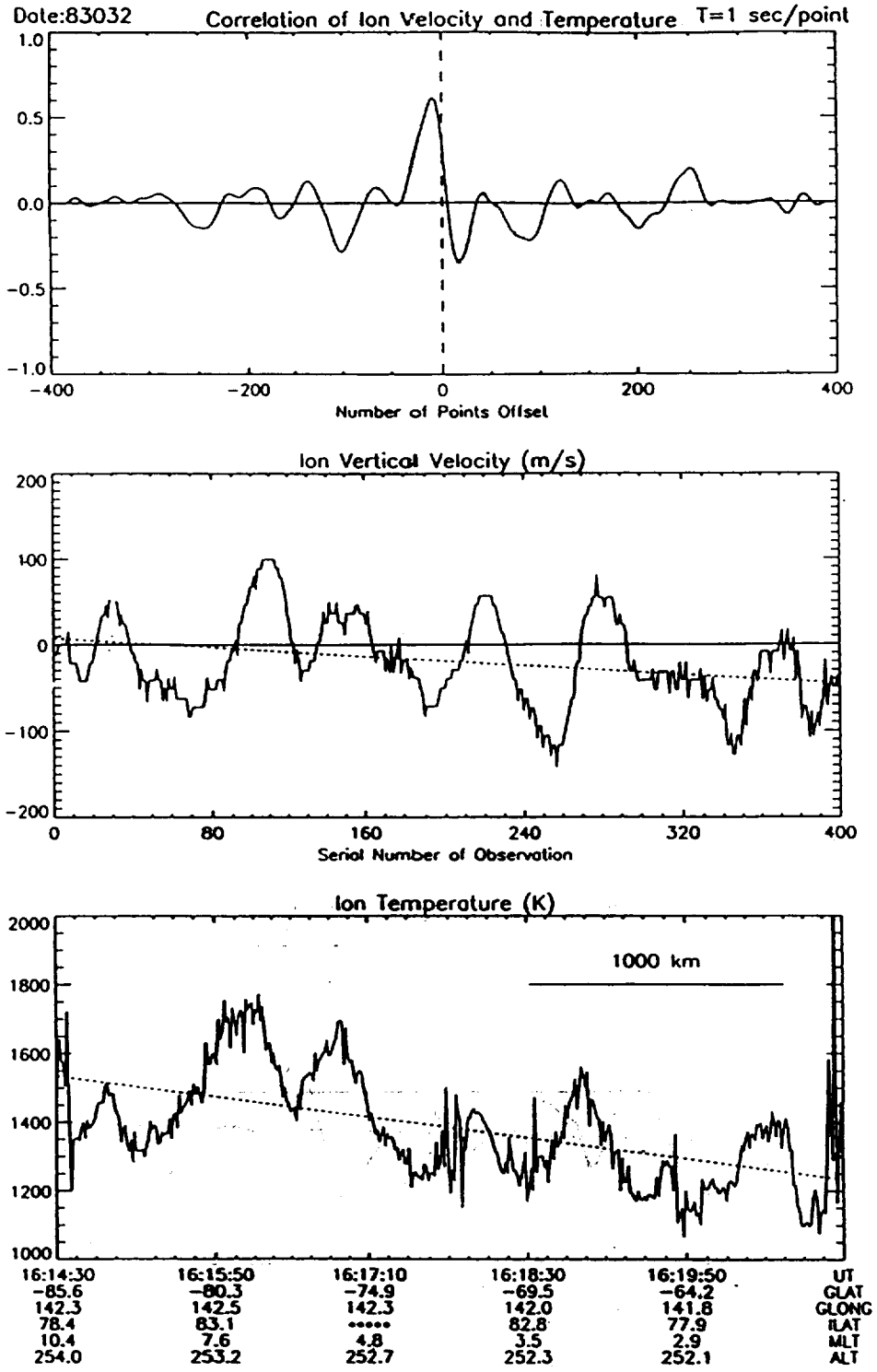

Figure 4. Part of the data presented in Figure 1 for 400 measurements of the ion vertical velocity and ion temperature over the polar cap, and the cross correlation between them. The dotted lines are the backgrounds from which perturbations were evaluated. The phase shift of nearly 90° is characteristic of propagating waves, and the fact that the velocity perturbation lags the temperature perturbation indicates that the horizontal wave progression is opposite to the direction of satellite motion; that is, propagation is from the nightside to the dayside.

vertical velocities are closely coupled, and there is striking observational evidence that this is so. As the magnetic field is nearly vertical, the observed ion vertical velocity components are essentially the field-aligned components of the neutral velocity. The correlation (i.e., the cross correlation at zero shift) between the ion and neutral velocity perturbations shown in Figures 4 and 5 is 0.93.

There is good evidence for the presence of horizontal neutral velocity perturbations associated with the waves, the horizontal perturbation velocities being about one-third as

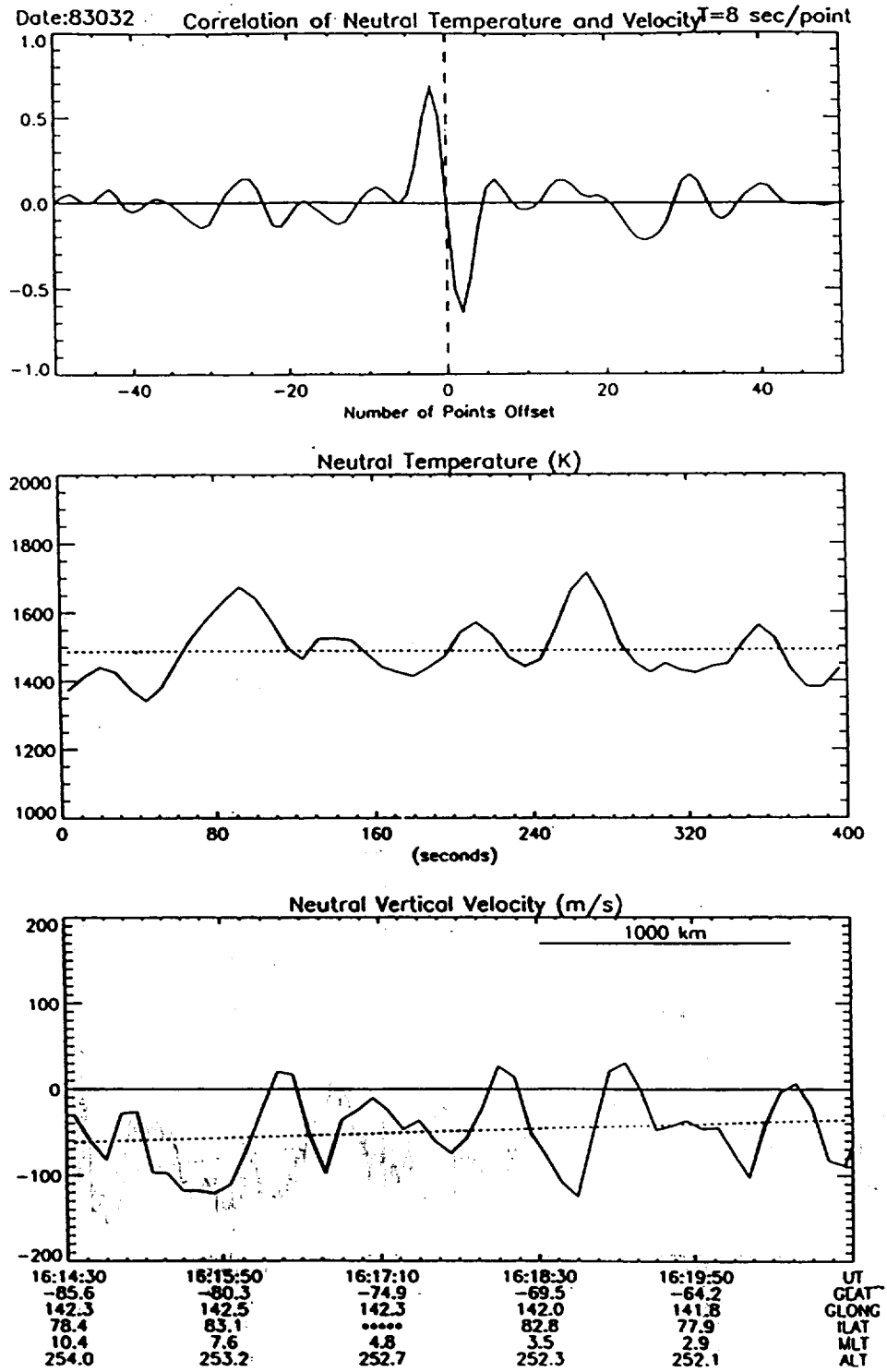

Figure 5. Neutral vertical velocities and temperatures plotted at 8-s intervals over the same time period covered by Figure 4, and the cross correlation between them. The dotted lines indicate the reference levels from which the perturbations were evaluated.

large as the vertical (e.g., orbits 1182, 1418, 1488, 4698, 4828, 6877, 8803). However, in many cases, no related perturbations in the horizontal neutral velocities could be seen; this might be due to the fact that only the component of the horizontal motion perpendicular to the orbit plane was observed; the perturbations may have been too small to recognize. Further, recognition of perturbations associated with the waves is made difficult by the presence of large horizontal winds with strong horizontal gradients, associated with anti-sunward convection over the polar cap, making it necessary to look for small perturbations on steep slopes.

The correlation (i.e., the cross correlation at zero shift) between the ion and neutral temperature perturbations shown in Figures 4 and 5 is 0.82. Although the ion and neutral temperature perturbations agree very well, the absolute values are often not in good agreement, probably reflecting

instrumental errors in one or both of the two instruments involved. The vertical velocity perturbations also agreed very well but the absolute values sometimes differed substantially; this was probably due to differences in the selection of the zero levels for the two instruments. However, the absolute values are not needed in the calculations of energy flux discussed below. Problems involving error in satellite orientation were ruled out for times comparable to the perturbation period by making use of magnetometer observations.

The wave period can be determined from the measured values of the amplitude of the vertical velocity component V_o and inferred values of the vertical displacement amplitude D_o by making use of the relationship for harmonic variations $\tau = 2\pi D_o / V_o$. The vertical displacement amplitudes were inferred from the observed temperature perturbations (assuming adiabatic temperature changes due to vertical displacements) and from the observed composition changes (assuming diffusion equilibrium in the unperturbed state and no changes in the composition of air parcels as a result of their vertical displacements from their unperturbed altitudes). The adiabatic lapse rate g/C_p at satellite altitude is about 7 K/km; thus a temperature change of ±100 K indicates a displacement amplitude of about 14 km. Combining this with a velocity amplitude of 100 m/s, the wave period is about 850 s, which is very close to the Brunt-Vaisala frequency at the satellite altitude; it could be larger or smaller than the Brunt Vaisala period. As horizontal wind perturbations are seen much of the time, the waves are presumably gravity waves with frequencies close to but below the Brunt-Vaisala frequency. The apparent horizontal wave length in the data is about 500 km, but this may be somewhat larger than the true value because the satellite velocity vector is not likely to be well aligned with the wave propagation vector. The horizontal phase velocity of the waves therefore is apparently something less than 500 m/s.

Another indication of the amplitude of vertical motion can be obtained from the observed composition variations, in particular the observed [O]/[Ar] and [N_2]/[Ar] ratios. Figure 6a shows these ratios for orbit 8303. The observed perturbation of the [O]/[Ar] ratio was ±260 about a mean value of 1000 at 1618 UT, indicating an altitude perturbation of about 13 km. The observed perturbation of the [N_2]/[Ar] ratio was ±60 about a mean value of 800, indicating an altitude perturbation of about 8 km. The corresponding figures for orbit 8036, shown in Figure 6b, are 1300 ±200 and 800 ±100, indicating vertical displacement perturbations of 10 and 13 km. Thus the composition variations indicate vertical displacement amplitudes of about 10 km or a little greater, in reasonably good agreement with the amplitudes inferred from the temperature perturbations. We also examined the [He]/[Ar] ratios, but these indicated displacements only about a quarter as great as those mentioned above. However, *Hodges* [1970] has shown that helium is not a good tracer for this purpose because of nonlinear transport effects by internal gravity waves; we have therefore not made any use of ratios involving helium concentrations.

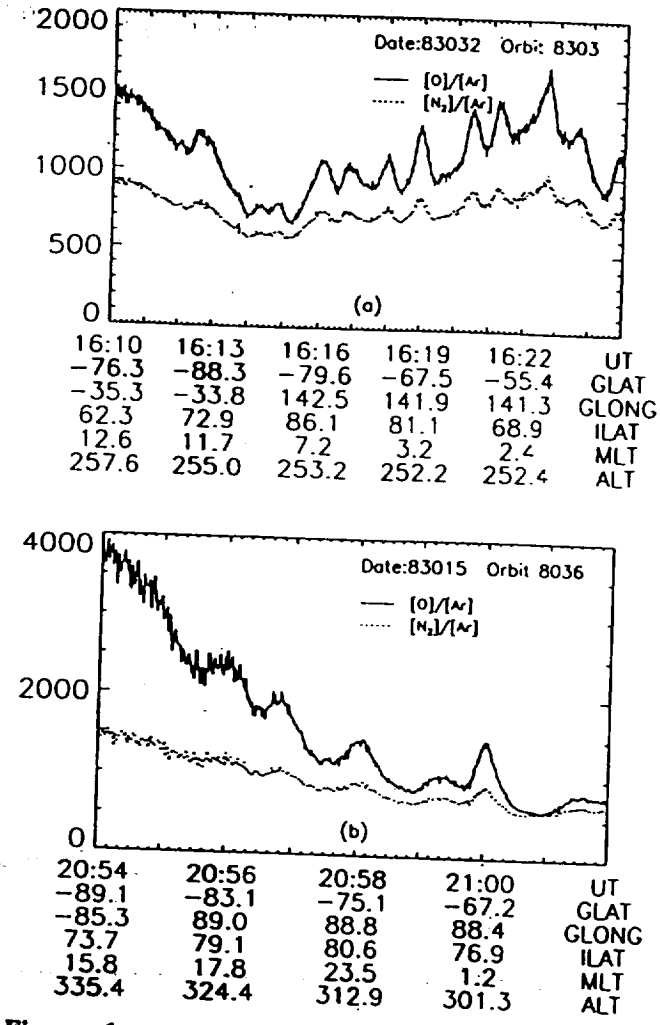

Figure 6. (a) The variations in the composition ratios [O]/[He] and [N_2]/[Ar] for orbit 8303, based on measurements by the NACS. (b) Similar data from orbit 8036.

Upward Energy Transport

Significant pressure variations associated with the waves under discussion occur at the satellite altitude. The top panel in Figure 7 shows the neutral pressures calculated from the composition and temperature measurements on orbit 8303. The second panel shows the pressure variations relative to a baseline or detrend curve drawn though the observed values as indicated by the dotted line in the top panel. The positive perturbations are nearly in phase with the vertical velocities shown in the third panel, thus indicating a component of energy flow in the vertical direction, as shown in the fourth panel. Where the vertical velocity perturbations are upwards, the pressure perturbations are positive (indicating upwards energy transport); where the vertical velocity perturbations are downwards, the pressure perturbations are negative (also indicating upwards energy transport). The upwards energy transport due to the waves is given by the product $\Delta v \Delta p$ of the vertical velocity perturbation Δv and the pressure perturbation Δp [*Sommerfeld*, 1964]. The calculations based on vertical velocities and pressures indicate a vertical component of energy flow averaged over the 400-s interval portrayed in the figure of 0.04 erg/cm^2-s. Curiously, this is about equal to the maximum rate of solar energy input above 250 km.

Figure 8 shows the calculated upward energy flux for five more orbits with altitudes ranging from about 310 to 560 km. The last two orbits, 6876 at 550 km and 6877 at 560 km, are very close to the exobase; the upward flow of energy is still substantial, although perhaps a factor or two or three less than

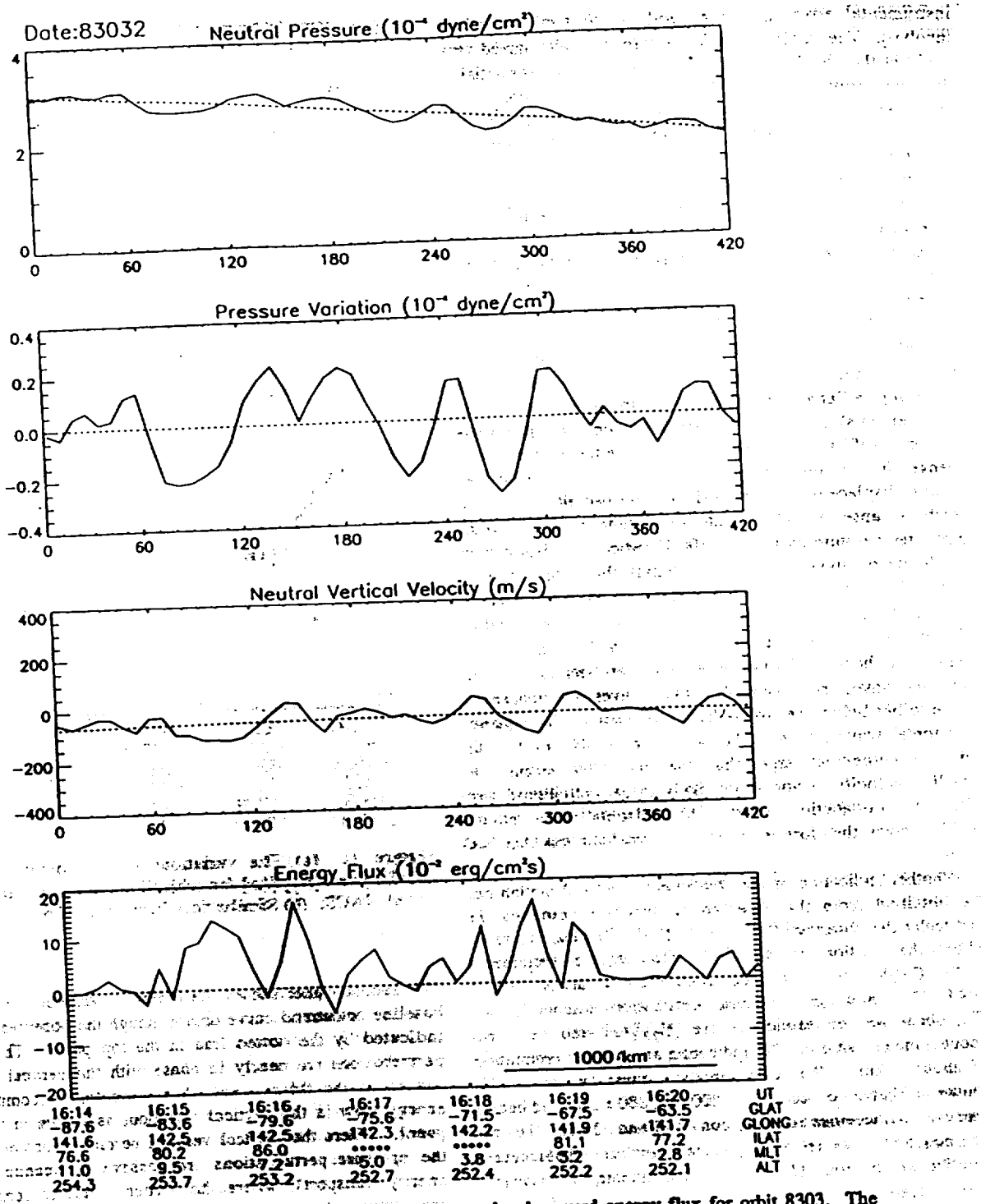

Figure 7. The neutral pressures and velocities and the associated upward energy flux for orbit 8303. The dotted lines in the top and third panels are the reference levels from which the perturbations were evaluated.

at lower altitudes. There was no convincing evidence that the temperature in the upper thermosphere was higher in the polar regions at the time of these observations. Hence the upward flow of energy at the times of these events is presumably balanced by an energy flow to lower latitudes associated with exospheric lateral transport.

Discussion

Fifty-one good records of polar cap gravity waves have been found and analyzed. These range in altitude from 250 to 560 km. In 41 cases the horizontal phase propagation of the waves clearly had a component from the nightside towards the dayside; none was observed propagating in the opposite sense. In the remaining 10 cases the orbit was near the terminator plane, and classification in a day-night sense was not possible; these cases were about equally divided between dawn-to-dusk and dusk-to-dawn for the sense of the propagation direction. In the 41 cases the waves tended to be of greater amplitude on the nightside. In some cases waves could be recognized only on the nightside, although in most

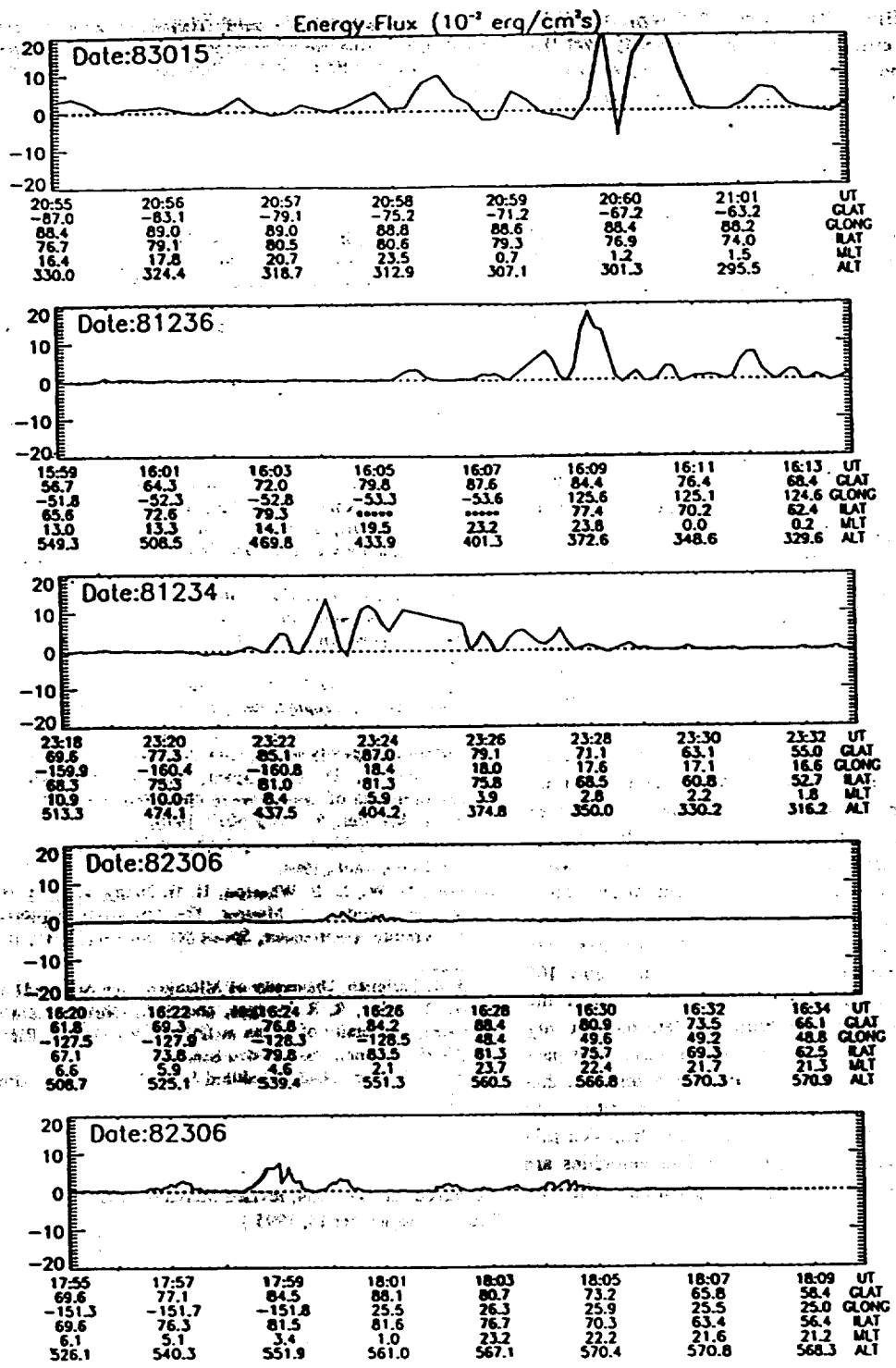

Figure 8. Five examples of upward energy flow due to waves at altitudes ranging from 310 to 560 km. Although the two highest orbits show lesser upward energy flow than those at lower altitudes, the upward component of energy flow falls off remarkably little with increasing altitude.

cases they extended all the way across the polar cap. In a few cases there was evidence that the waves extended a short distance beyond the polar cap on the dayside.

A troubling observation is that some examples have been found that have clear wave signatures in terms of vertical ion velocities but without recognizable accompanying ion temperature perturbations. It is a characteristic of standing waves that the displacements be zero when the velocity perturbations have their maximum values, so there is some temptation to suggest that such observations are indicative of standing waves. However this hypothesis seems not to be tenable, in that we have found no cases showing clear temperature signatures in the absence of clear signatures in vertical velocity, something that should be observed with equal frequency for standing waves.

Finally, it is important to note that the closeness of the

wave frequency to the Brunt-Vaisala frequency ω_B, as well as the dominance of the vertical component of velocity over the horizontal velocity in the observed wave structures, are natural consequences of the dispersion of gravity waves in the upper thermosphere. Throughout much of the thermosphere the temperature increases with increasing altitude; this causes ω_B to decrease with altitude. In the plane wave approximation, Snell's law requires that the horizontal component of the wave number be invariant with altitude. *Lamb* [1945] showed that the effective vertical component of the wave number decreases with increasing temperature, reaching zero at the level where $\omega_B = \omega$, and evanescent beyond. Hence the decay of ω_B with increasing altitude in the thermosphere imposes a low-pass filter with decreasing cutoff frequency on the spectrum of gravity wave oscillations.

The prevalence of observable wave structures near the Brunt-Vaisala frequency is apparently owed to the resonance condition as ω_B approaches , which corresponds to a match of the wave frequency with the natural frequency of buoyant oscillations of gas parcels. The width of this resonance is made finite by viscous dissipation, and gravity waves excited by impulsive natural phenomena have a broad spectrum of frequencies. As a result, wave-induced atmospheric perturbations over a band of wave frequencies near but below ω_B are selectively amplified by the resonance, creating a quasi-sinusoidal structure in which the lower-frequency components of the wave spectrum are suppressed.

In quasi-resonant oscillations near the Brunt-Vaisala frequency the dominance of vertical motion seems obvious. An analytic explanation can be found in Figure 3 of *Midgley and Liemohn* [1966], which shows how the orbits of gas parcels in acoustic-gravity waves change with wave parameters. What is of interest to the present discussion is that the orbits are elliptical, with the major axis nearly vertical near the condition $\omega_B = \omega$. As ω_B increases with decreasing altitude below about 250 km down to below 100 km, the major axis of the orbit ellipse tilts toward the horizontal. Hence the large amplitude oscillations near ω_B that predominate above 250 km are rooted in waves that pass through lower altitudes with very classical characteristics, that is, with horizontal velocities greater than the vertical. At altitudes above about 250, above which the Brunt-Vaisala frequency changes relatively little, the vertical velocities are naturally greater than the lateral, in agreement with the velocity measurements.

Acknowledgments. We thank Tianyang Ding for his assistance with data analysis. This work was supported in part by NASA grant NAGW-4002, by F19628-93-K-0008 Phillips Laboratory, and by the Cecil and Ida Green Honors Chair.

The Editor thanks three referees for their assistance in evaluating this paper.

References

Carignan, G. R., B. P. Block, J. C. Maurer, A. E. Hedin, C. A. Reber, and N. W. Spencer, The neutral mass spectrometer on Dynamics Explorer, *Space Sci. Instrum.*, 5, 429, 1981.

Gross, S. H., and F. T. Huang, Medium scale gravity waves in the thermosphere observed by the AE-C satellite, IEEE Trans. *Geosci. Remote Sens., GE-23, No. 4*, 139-149, March, 1985.

Hanson, W. B., R. A. Heelis, R. A. Power, C. R. Lippincott, D. R. Zuccaro, B. J. Holt, L. H. Harmon, and S. Sanatani, The retarding potential analyzer for Dynamics Explorer-B, *Space Sci. Instrum.*, 5, 503, 1981.

Heelis, R. A., W. B. Hanson, C. R. Lippincott, D. R. Zuccaro, L. H. Harmon, B. J. Holt, J. E. Doherty, and R. A. Power, The ion drift meter for Dynamics Explorer-B, *Space Sci. Instrum.*, 5, 511, 1981.

Hodges, R. R., Jr., Eddy diffusion coefficients due to instabilities in internal gravity waves, *J. Geophys. Res.*, 74, 4087-4090, 1969.

Hodges, R. R., Jr., Vertical transport of minor constituents in the lower thermosphere by nonlinear processes of gravity waves, *J. Geophys. Res.*, 75, 4842-4847, 1970.

Lamb, H., *Hydrodynamics*, 6th ed., chap. X, Dover, Mineola, N. Y., 1945.

Midgley, J. E., and H. B. Liemohn, Gravity waves in a realistic atmosphere, *J. Geophys. Res.*, 71, 3729-3748, 1966.

Pitteway, M. L. V., and C. O. Hines, The viscous damping of atmospheric gravity waves, *Can. J. Phys.*, 41, 1935-1948, 1963.

Potter, W. E., D. C. Kayser, and K. Mauersberger, Direct measurements of neutral wave characteristics in the thermosphere, *J. Geophys. Res.*, 81, 5002-5012, 1976.

Sommerfeld, A., *Mechanics of Deformable Bodies*, chap. 5, Academic, San Diego, Calif., 1964.

Spencer, N. W., L. E. Wharton, H. B. Niemann, A. E. Hedin, G. R. Carignan, and J. C. Maurer, The Dynamics Explorer wind and temperature spectrometer, *Space Sci. Instrum.*, 5, 417, 1981.

G. R. Carignan, University of Michigan, Ann Arbor, MI 48109-2116

W. R. Coley, R. R. Hodges, and F. S. Johnson, Center for Space Sciences, University of Texas at Dallas, Box 830688, Richardson, TX 75083-0688 (e-mail: cssmail@utdsss.edu)

N. W. Spencer, NASA Goddard Space Flight Center, Greenbelt, MD 20771.

(Received July 19, 1994; revised March 6, 1995; accepted September 14, 1995.)